
This is an electronic reprint of the original article.

This reprint may differ from the original in pagination and typographic detail.

Author(s): Jood, P. & Peleckis, G. & Wang, X. L. & Dou, S. X. & Yamauchi, H. & Karppinen, Maarit

Title: Phase formation and magnetotransport of alkali metal doped Na_{0.75}CoO₂ thermoelectric oxide

Year: 2010

Version: Final published version

Please cite the original version:

Jood, P. & Peleckis, G. & Wang, X. L. & Dou, S. X. & Yamauchi, H. & Karppinen, Maarit. 2010. Phase formation and magnetotransport of alkali metal doped Na_{0.75}CoO₂ thermoelectric oxide. Journal of Applied Physics. Volume 107, Issue 9. 09D716/1-3. ISSN 0021-8979 (printed). DOI: 10.1063/1.3365491.

Rights: © 2010 AIP Publishing. This is the accepted version of the following article: Jood, P. & Peleckis, G. & Wang, X. L. & Dou, S. X. & Yamauchi, H. & Karppinen, Maarit. 2010. Phase formation and magnetotransport of alkali metal doped Na_{0.75}CoO₂ thermoelectric oxide. Journal of Applied Physics. Volume 107, Issue 9. 09D716/1-3. ISSN 0021-8979 (printed). DOI: 10.1063/1.3365491, which has been published in final form at <http://scitation.aip.org/content/aip/journal/jap/107/9/10.1063/1.3365491>.

Phase formation and magnetotransport of alkali metal doped Na_{0.75}CoO₂ thermoelectric oxide

P. Jood, G. Peleckis, X. L. Wang, S. X. Dou, H. Yamauchi, and M. Karppinen

Citation: *Journal of Applied Physics* **107**, 09D716 (2010); doi: 10.1063/1.3365491

View online: <http://dx.doi.org/10.1063/1.3365491>

View Table of Contents: <http://scitation.aip.org/content/aip/journal/jap/107/9?ver=pdfcov>

Published by the AIP Publishing

Articles you may be interested in

Tuning the functional properties of PMN-PT single crystals via doping and thermoelectrical treatments
J. Appl. Phys. **114**, 224112 (2013); 10.1063/1.4847975

Influence of rare earth doping on thermoelectric properties of SrTiO₃ ceramics
J. Appl. Phys. **114**, 223714 (2013); 10.1063/1.4847455

Effect of electron doping on thermoelectric properties for narrow-bandgap intermetallic compound RuGa₂
J. Appl. Phys. **113**, 023713 (2013); 10.1063/1.4775602

Cosubstitution effect on the magnetic, transport, and thermoelectric properties of the electron-doped perovskite manganite CaMnO₃
J. Appl. Phys. **108**, 103702 (2010); 10.1063/1.3505756

Thermal conductivity of the thermoelectric layered cobalt oxides measured by the Harman method
J. Appl. Phys. **96**, 931 (2004); 10.1063/1.1753070

The new SR865 2 MHz Lock-In Amplifier ... \$7950




Chart recording FFT displays Trend analysis

Features

- Intuitive front-panel operation
- Touchscreen data display
- Save data & screen shots to USB flash drive
- Embedded web server and iOS app
- Synch multiple SR865s via 10 MHz timebase I/O
- View results on a TV or monitor (HDMI output)

Specs

- 1 mHz to 2 MHz
- 2.5 nV/√Hz input noise
- 1 μs to 30 ks time constants
- 1.25 MHz data streaming rate
- Sine out with DC offset
- GPIB, RS-232, Ethernet & USB

SRS Stanford Research Systems
www.thinksrs.com • Tel: (408)744-9040

Phase formation and magnetotransport of alkali metal doped $\text{Na}_{0.75}\text{CoO}_2$ thermoelectric oxide

P. Jood,¹ G. Peleckis,^{1,a)} X. L. Wang,¹ S. X. Dou,¹ H. Yamauchi,² and M. Karppinen²

¹*Institute for Superconducting and Electronic Materials, University of Wollongong, Wollongong, New South Wales 2519, Australia*

²*Laboratory of Inorganic and Analytical Chemistry, Helsinki University of Technology, FIN-02015, Finland*

(Presented 19 January 2010; received 30 October 2009; accepted 30 November 2009; published online 21 April 2010)

Synthesis and characterization of bulk Na_xCoO_2 samples substituted by K and Rb is reported. Phase formation studies revealed a narrow stable region for Na-alkali metal-Co system. Whisker and platelike single crystalline structures have been found to form on the surface of the pellets in case of K doping. All samples were metallic and no characteristic anomaly in R-T curves was observed for Rb doped sample. Magnetoresistance measured has a pronounced positive response only for K-doped and pure Na_xCoO_2 phases, reaching 11% and 7% at 5 K temperature, respectively. © 2010 American Institute of Physics. [doi:10.1063/1.3365491]

In recent years constantly growing concern over decreasing amount of primary energy sources has prompted widespread research on development of alternative techniques and materials for power generation. Waste heat from power plants, factories, or automobiles equals to 70% of the total primary energy, but it is difficult to use as its sources are highly dispersed and small in size. The only effective method of overcoming these problems by converting heat energy directly into electrical energy is thermoelectric (TE) power generation. Good TE material should possess high conversion efficiency, be built out of nonvolatile and nontoxic elements, highly abundant and most important chemically stable at temperatures as high as 1000 K in air. Thus, oxide based TE materials are most promising candidates for TE applications due to their stability at high temperatures in air.

After Terasaki *et al.*¹ have reported that Na_xCoO_2 compound exhibits simultaneously high TE power and low resistivity ($S \approx 100 \mu\text{V/K}$ and $\rho \approx 200 \mu\Omega \text{ cm}$ at 300 K), many researchers put a lot of effort to develop new Co-based oxides that would exhibit similar or even better TE properties. Among many Co-based compounds three types of layered cobalt oxides have attracted the highest attention: Na_xCoO_2 , $\text{Ca}_3\text{Co}_4\text{O}_9$,² $\text{Bi}_2\text{Sr}_3\text{Co}_2\text{O}_9$.³ In Na_xCoO_2 TE oxide the sodium layers are sandwiched between CoO_2 blocks and these are stacked along the *c* axis. CoO_2 layers are responsible for electrical conductivity and Seebeck coefficient while the Na layers are insulating and determine thermal conductivity of the oxide. Fouassier *et al.*⁴ reported that a large amount of vacancies can easily be introduced into the sodium layer, giving a possibility for a high Na nonstoichiometry. It was also shown that highly sodium deficient and water intercalated $\text{Na}_x\text{CoO}_2 \cdot y\text{H}_2\text{O}$ is superconducting at low temperatures.⁵ Moreover, Balsys *et al.*⁶ reported that due to the peculiar layered structure, Na ions can freely migrate in between the oxygen layers. Such migration of Na ions might

be responsible for structural phase transitions close to room temperature which were described by Tojo *et al.*⁷ They have found existence of three first order transitions at 288.7, 296.3, and 302.1 K. This result is supported by Motohashi *et al.*,⁸ who showed anomalous behavior in electrical resistivity curves for Na_xCoO_2 polycrystalline samples.

As being a transition metal oxide, Na_xCoO_2 is very attractive for chemical substitution studies. Both cation sites, Na and Co, can be substituted by various elements. Kawata *et al.*⁹ showed enhanced TE properties for Ca-substituted samples. On the other hand Sr does not go into Na site, but forms an individual compound Sr_xCoO_2 .¹⁰ Other studies showed that Mn, Ru, and Rh act as strong scatters to increase electrical resistivity rapidly, while Cu, Zn, and Pd substitution does not alter the electric conduction.^{11,12} In this article we present synthesis and characterization of alkali metal doped $\text{Na}_x\text{R}_y\text{CoO}_2$ ($R=\text{K}, \text{Rb}$) polycrystalline samples. The introduction of bigger alkali metal ions might decrease Na migration in the layer and thus improve transport properties of the material.

All samples were prepared applying “rapid heat-up” technique.⁸ Phase purity was checked using x-ray powder diffraction (MAC Science, MXP18VAHF, $\text{Cu K}\alpha_1$ radiation). Phase formation was studied by means of thermogravimetric (TG) analysis (Perkin Elmer, Pyris 1). For full synthesis simulation, a 5–30 mg amount of sample was put into the thermobalance. In order to avoid fast alkali metal evaporation, the heating rate of 2°C/min was adopted. The morphology and microstructure of the samples was investigated by scanning electron microscopy (SEM) (Hitachi, S-4500). Chemical composition of the samples was determined using inductively coupled plasma atomic emission spectrometer (ICP-AES) (Seiko, SPS1500VR). Transport properties were analyzed by physical property measurement system (Quantum Design) in a temperature range of 5–350 K. For magnetoresistance studies the applied field was varied from 0 to 7 T.

^{a)}Author to whom correspondence should be addressed. Electronic mail: peleckis@uow.edu.au.

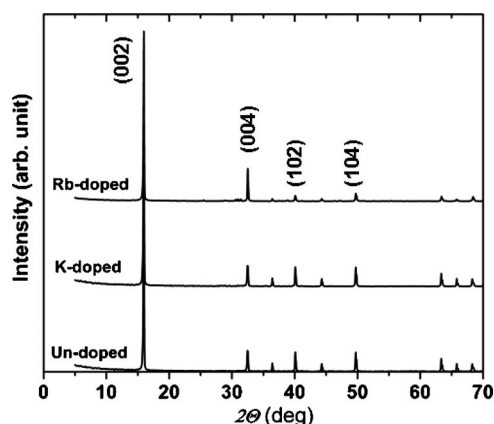


FIG. 1. X-ray diffraction patterns for sintered $\text{Na}_x\text{R}_y\text{CoO}_2$ ($\text{R}=\text{K},\text{Rb}$) samples.

Figure 1 shows x-ray diffraction patterns of undoped and K/Rb doped Na_xCoO_2 samples after sintering. The samples are of single phase corresponding to that of hexagonal $\gamma\text{-Na}_{0.75}\text{CoO}_2$ oxide. The 002 and 004 peaks at $2\theta=16.2^\circ$ and 33.4° are much higher in intensity for the Rb doped sample as opposed to other ones indicating a more pronounced c axis orientation. Lattice parameters calculated from the x-ray diffraction patterns revealed that introduction of bigger alkali ion in the system caused elongation of the lattice parameter c , i.e., $c_{(\text{un-doped})}=10.912 \text{ \AA}$ and $c_{(\text{Rb-doped})}=10.946 \text{ \AA}$, respectively.

Figures 2(a) and 2(b) show SEM micrographs of $\text{Na}_{0.75}\text{Rb}_{0.25}\text{CoO}_2$ calcined powders and sintered pellets, respectively. As we can see, the sample morphology has very distinctive differences. For calcined powders the particles are embedded in some sort of melt and the shape of the particles is somewhat circular. In contrary, the particles in the sintered sample [Fig. 2(b)] are well formed and separated, have clear signs of layered structure, and are elongated in shape. Some residue of melting or sublimation can be seen on the surface of the crystallites. The average particle size is about $20 \mu\text{m}$. Furthermore, it was found that for K-doped samples, single crystalline like formations have been observed [Fig. 2(c)]. Two kinds of distinctive products were formed: whisker-type and petal-like crystals [as indicated in Fig. 2(c)]. The formation of the product was found to be highly dependant on K amount in the samples and sample sintering temperature, i.e., higher K content and higher temperatures caused larger amount of petal-like crystals to be formed. Detailed phase formation analysis and TE properties of whisker type crystals is reported elsewhere.¹³ We were unable to measure electric properties of petal like crystals as they were very brittle and thin.

To establish and understand the proper synthesis procedure we have performed TG simulation of synthesis procedure. Figure 3 shows TG curve for the simulation of solid-state reaction, when Rb is doped into Na_xCoO_2 sample. The TG curve has distinctive difference as compared to published data for Na-pure samples.⁸ At around $600\text{--}700^\circ\text{C}$ we have stable triple cation system, i.e., Na–Rb–Co. However, we can see a drop in weight at temperatures above 760°C . This can be attributed to the evaporation of Rb from the samples. At

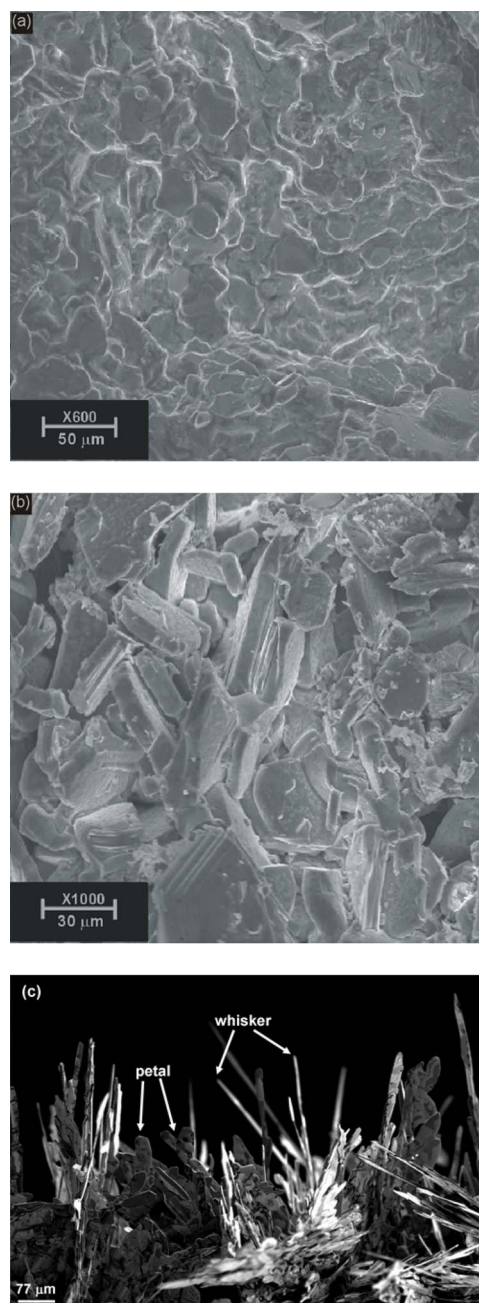


FIG. 2. (Color online) SEM pictures of (a) calcined, (b) sintered $\text{Na}_{0.75}\text{Rb}_{0.25}\text{CoO}_2$ samples, and (c) single crystalline products on the surface of the pellets for K-doped samples.

temperature of 830°C almost half of Rb content is already lost and is completely vanished at 860°C . This is in contrast to K-doped samples, where stable Na–K–Co temperature region is broader, i.e., $650\text{--}830^\circ\text{C}$.¹³ The observed Rb evaporation is supported by ICP-AES results, which showed that $\text{Na}_{0.75}\text{Rb}_{0.25}\text{CoO}_2$ precursor powders [region between steps (2) and (3)] after sintering [after step (3)] were in fact $\text{Na}_{0.73}\text{Rb}_{0.02}\text{CoO}_2$.

Electrical properties measured revealed that all samples are metallic, with lowest electrical resistivity (ρ) at 300 K for Rb substituted $\text{Na}_{0.75}\text{CoO}_2$, i.e., $\rho=0.9 \text{ m}\Omega \text{ cm}$. The Rb doped sample does not show characteristic anomaly in the electrical resistivity curve at room temperature which is in contrast to undoped⁸ $\text{Na}_{0.75}\text{CoO}_2$. Furthermore, we have in-

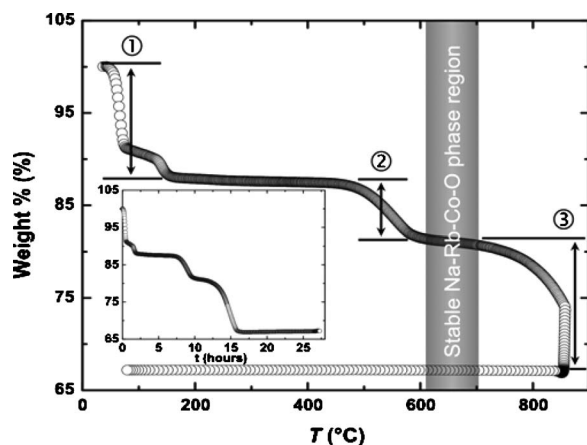


FIG. 3. TG curve of a raw material powder mixture (Na:Rb:Co = 0.75:0.25:1) upon heating in O_2 gas. (① Evaporation of H_2O ; ② decarbonation process; and ③ depletion of Rb.) Inset shows the same data with respect to time.

investigated magnetotransport properties of our samples at 5 K [Fig. 4(b)]. The undoped sample shows positive magnetoresistance (MR) effect reaching 11% at 5 K. In the case of K doping this MR response is suppressed to 7%. Lastly, for Rb doped sample the MR effect is positive and negative, yet quite small, i.e., $\sim 4\%$. The origin of such suppression of the

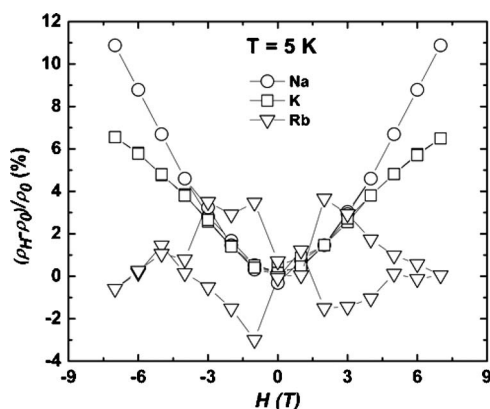


FIG. 4. MR for pure and alkali metal doped $Na_{0.75}CoO_2$ measured at 5 K.

MR effect might be related to the structural reordering and elongation of lattice parameter c . It is possible that due to the longer distances between CoO_2 layers, the magnetic ordering in the material is lower than that for undoped compound.

In summary, K and Rb doped samples of $Na_{0.75}CoO_2$ TE oxide were prepared via “rapid heat-up” synthesis technique. Single crystalline structures were observed on the surface of the pellets for K-doped samples. TG analysis showed depletion of doped alkali ion during sintering procedure. All samples were metallic with positive MR effect for undoped and K-doped samples reaching 11% and 7% at 5 K, respectively. In contrast, Rb doped sample showed weakly pronounced MR features which might be caused by significant structural/microstructural changes.

ACKNOWLEDGMENTS

G.P. thanks the Australian Research Council for support under Discovery Grant No. DP0 879 714. P.J. thanks the University of Wollongong for providing matching scholarship for her Ph.D. studies.

- ¹I. Terasaki, Y. Sasago, and K. Uchinokura, *Phys. Rev. B* **56**, R12685 (1997).
- ²A. C. Masset, C. Michel, A. Magnan, M. Hevein, O. Oulemonde, F. Studier, and B. Raveau, *Phys. Rev. B* **62**, 166 (2000).
- ³J. M. Tarascon, R. Rajesh, P. Darboux, M. S. Hedge, G. W. Hull, L. H. Greene, M. Giroux, Y. Lesage, W. R. McKinnon, J. V. Waszczak, and L. F. Schneemeyer, *Solid State Commun.* **71**, 663 (1989).
- ⁴C. Fouassier, G. Matejka, J.-M. Reau, and P. Hagenmuller, *J. Solid State Chem.* **6**, 532 (1973).
- ⁵K. Takada, H. Sakurai, E. Takayama-Muromachi, F. Izumi, R. A. Dilanian, and T. Sasaki, *Nature (London)* **422**, 53 (2003).
- ⁶R. J. Balsys and R. L. Davis, *Solid State Ionics* **93**, 279 (1997).
- ⁷T. Tojo, H. Kawaji, T. Atake, Y. Yamamura, M. Hashida, and T. Tsuji, *Phys. Rev. B* **65**, 052105 (2002).
- ⁸T. Motohashi, E. Naujalis, R. Ueda, K. Isawa, M. Karppinen, and H. Yamauchi, *Appl. Phys. Lett.* **79**, 1480 (2001).
- ⁹T. Kawata, Y. Iguchi, T. Itoh, K. Takahara, and I. Terasaki, *Phys. Rev. B* **60**, 10584 (1999).
- ¹⁰R. Ishikawa, Y. Ono, Y. Miyazaki, and T. Kajitani, *Jpn. J. Appl. Phys., Part 2* **41**, L337 (2002).
- ¹¹R. Kitawaki and I. Terasaki, *J. Phys.: Condens. Matter* **14**, 12495 (2002).
- ¹²S. Li, R. Funahashi, I. Matsubara, and S. Sodeoka, *Mater. Res. Bull.* **35**, 2371 (2000).
- ¹³G. Peleckis, M. Karppinen, and H. Yamauchi, *Appl. Phys. Lett.* **83**, 5416 (2003).